NASA Contractor Report 172364

SINGLET OXYGEN GENERATOR FOR A SOLAR
POWERED CHEMICALLY PUMPED IODINE LASER

George E. Busch

KMS FUSION, INC.
Ann Arbor, Michigan 49106

NASA

National Aeronautics and
Space Administration

Langley Research Center
Hampton, Virginia 23665

PROJECT SUMMARY

Atomic iodine is used successfully as the active element in high power lasers operating at 1.3 micron wavelengths. The iodine laser transition is efficiently pumped by molecular oxygen in its singlet delta excited state. The objective of this research was to investigate and evaluate a method for generating singlet oxygen (O_2) gas directly from solid-phase material.

Thin films of a substituted naphthalene endoperoxide were pulse heated and the release of $O_2{}^1\Delta$ was monitored through its dimol emission at 634 nm. The time profile of the dimol emission was successfully modeled with a simple numerical code which also aided in determinations of absolute specific yield of $O_2{}^1\Delta$ released. These studies demonstrated that $O_2{}^1\Delta$ can be released into the gas phase in high yields ($\sim 100\%$) upon thermolysis of the endoperoxide. Furthermore, $O_2{}^1\Delta$ can be quantitatively released from thin films of endoperoxide in time scales as short as a millisecond.

In an integrated system, singlet oxygen generation is proposed as a three-step process in which certain triplet sensitizers convert ground-state oxygen to singlet oxygen by absorption of solar energy. The singlet oxygen oxidizes an appropriate acceptor molecule to form an endoperoxide which serves to trap and concentrate the singlet oxygen. For subsequent release of the stored oxygen, the endoperoxide is thermally decomposed, generating $O_2{}^1\Delta$ in the gas phase and leaving the original acceptor molecule for recycling. The overall energy conversion efficiency from sunlight to laser light is potentially greater than 10%. The results of the Phase I research program demonstrate that step three of this three-step process can be very efficienct. Steps one and two will be addressed in future studies.
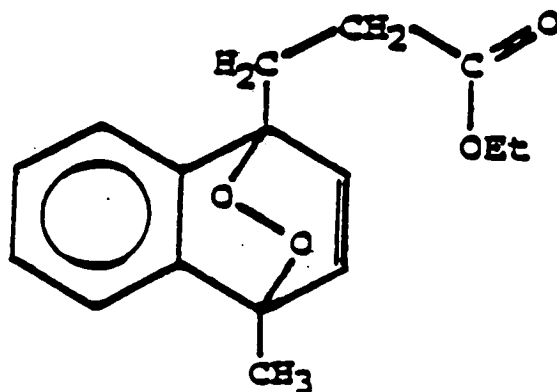
N84-28899

PROJECT OBJECTIVES

The Phase I objective was to determine the potential of solid phase endoperoxides as a means to produce singlet oxygen in the gas phase in concentrations useful to chemical lasers. Questions of whether quenching could be held to acceptable levels and whether sufficient $O_2{}^1\Delta$ evolution rates could be achieved were to be addressed. Perhaps the full potential of endoperoxides for $O_2{}^1\Delta$ production has not yet been determined, but yields approaching 100% have been demonstrated for thin films of solid endoperoxide. This has been accomplished on short time scales (~ 1 ms) and thus many of the questions about problems of quenching and achievable $O_2{}^1\Delta$ evolution rates have been put to rest.

DETAILS OF PHASE I RESEARCH

Release of $O_2{}^1\Delta$ from solid endoperoxide was observed with the experimental apparatus shown in Figure 1. An endoperoxide coated Nesatron plate (PPG Industries) was mounted in full view of a photomultiplier tube. An interference filter with a 10 nm bandpass centered near 634 nm spectrally limited the light passing to the photomultiplier to only those wavelengths in the neighborhood of the $O_2{}^1\Delta$ dimol emission.

The 1,4-endoperoxide of ethyl 3-(4-methyl-1-naphthyl) propanoate

was deposited on the indium oxide layer of a 5 cm square Nesatron glass plate (see Figure 1) by spin coating. Typical surface densities of endoperoxide

2

ranged from 5×10^{15} to 4×10^{16} molecules/cm^2 depending on the concentration of the spin coat solution. Assuming a film mass density of 1.2 g/cm^3, film thicknesses of 15 nm to 120 nm are calculated. Surface densities were measured by redissolving a deposited film in a known volume of solvent, allowing the solution to sit at room temperature overnight for the conversion of endoperoxide to naphthalene, and finally measuring the optical absorption of the solution at 290 nm where naphthalene absorption is prominent.

Singlet delta oxygen was released from the endoperoxide upon heating the organic film. The endoperoxide was rapidly heated by discharging a bank of capacitors (100 to 400 microfarad, charged to voltages between 400v and 660v) through the conductive indium oxide coating of the Nesatron plate. Because the endoperoxide film was thin and in intimate contact with the indium oxide layer, the temperature of the endoperoxide film tracked the surface temperature of the Nesatron plate. In all cases, the indium oxide layer and the deposited endoperoxide layer were thin compared to thermal diffusion distances in the glass substrate on a millisecond time scale.

For the case of a surface heat source delivering energy to the plate at a rate which is decaying exponentially in time, the time dependence of temperature on the surface of the plate should follow the expression

$$T_s(t) = \frac{\hat{E}}{K \tau} \frac{(D\,\tau)^{1/2}}{(\pi)^{1/2}} \int_0^1 \frac{e^{-(t/\tau)x}}{(1-x)^{1/2}} dx \tag{1}$$

in which D is the thermal diffusivity of the glass substrate, K is the thermal conductivity, $\hat{E}$ is the energy stored on the capacitor bank per unit area of the glass substrate, and τ is the time constant for energy discharge. Equation (1) is plotted in Figure 2 for the time dependence of the surface temperature of a Nesatron plate during the discharge of a 200 µf capacitor charged to 600v.

Experimental Results

The dimol emission signal at 634 nm for a typical experiment is shown in Figure 3, which displays a scope trace of the photomultiplier output vs. time. The time constant for the detection system is ~ 0.3 ms, while that for

3

the energy discharge is ~ 1.6 ms. Dimol emission signals were surprisingly reproducible from sample to sample implying good control of the film thickness with the spin coating technique.

The decay of the dimol emission signal seen in Figure 3 was initially thought to be due to quenching reactions. However, it was soon realized that diffusion at atmospheric pressures would contribute to the apparent signal decay since dimol emission intensity is second order in $O_2{}^1\Delta$ concentration. A computer model was developed which simulates the emission signal quite well and will be more fully discussed in the following section.

Since only 10% or less of the total light being emitted from the heated endoperoxide samples was being transmitted by the interference filter, an emission spectrum was sought to verify that $O_2{}^1\Delta$ dimol emission was indeed being observed, and not some accidental overlap with emission from unantici- pated species.

Although signal to noise ratios were good using the experimental set-up of Figure 1, emission is sufficiently weak that attempts to spectrally resolve the light required the special measures shown in Figure 4. First, the direct viewing of the plate done in Figure 1 was replaced by an integrating cell com- prised of two plexiglass plates coated inside with highly reflective $BaSO_4$. A slit 1 mm wide by 1 cm high was cut in one face and this was imaged into the input slit of an f/4 spectrograph. The output of the spectrograph was directly coupled to an image intensifier (gain 10^4- 10^5) and the image intensifier output was coupled with an f/1.5 lens to a silicon intensifier target (SIT) vidicon tube. The results were recorded on video tape and subsequently fed to an image processor for signal averaging.

A spectrum recorded with the set-up of Figure 4 is displayed in Figure 5. Two peaks are shown: one at 634 nm corresponding to dimol emission to the ground vibrational state of each molecule, and one at 700 nm for emission to the state with one molecule vibrationally excited.

The peaks of Figure 5 are rotationally broadened significantly beyond the 20 nm resolution of the instrumentation. The positions of the calibration

lines in the upper panel of Figure 5 were obtained by recording a 633 nm HeNe laser line at spectrometer settings: 592, 633, and 700 nm. No evaluation has been made as to whether the magnitude of broadening of the spectral lines at 634 and 700 nm is reasonable for the temperature range 300-500° K. The possibility of contributions of uv light from higher diffraction orders of the grating was eliminated by using a 570 nm cutoff filter. The spectrum in Figure 5 is also in qualitative agreement with the 634 nm interference filter experiments using the configuration in Figure 1, in which it was observed that the 10 nm bandpass, 59% peak transmission filter reduced signals by about a factor of 10-12 from experiments with the filter removed.

Model Calculations

The decay of the dimol emission signal observed in Figure 3 is primarily due to diffusion. The intensity of emission seen by the photmultipler tube is proportional to the concentration of $O_2{}^1\Delta$ squared and integrated over the distance from the generating surface,

$$I \propto \int_0^\infty C^2(x, t) \, dx$$

At times large compared with the duration over which $O_2{}^1\Delta$ is released into the gas phase, the $O_2{}^1\Delta$ concentration can be approximated by

$$C(x,t) = (P_o \, e^{-x^2/4Dt})/(D \pi t)^{1/2},$$

the concentration expected at time t, a distance x from the generating surface. P_o is the number of singlet delta oxygen molecules per unit area instantaneously released at the generating surface at time t = 0. Performing the integral over space gives a dimol emission signal,

$$I \propto P_o{}^2/(2 \pi Dt)^{1/2},$$

which diminishes with the square root of time. Here D is the diffusion coefficient of $O_2{}^1\Delta$ in air (considered the same as that for ground state oxygen).

5

This analysis is not expected to accurately calculate the dimol emission signal at times comparable to the $O_2{}^1\Delta$ release time. It also fails to account for the energy pooling reaction which can be important at early times when the $O_2{}^1\Delta$ density is large. The energy pooling reaction may also reduce the number of $O_2{}^1\Delta$ molecules (P_0) which diffuse away and contribute to the signal at later times. Because of these considerations we developed a computer code which more accurately models the dimol emission signal. The one dimensional diffusion equation,

$$\frac{\partial c}{\partial t} = D \frac{\partial^2 c}{\partial x^2}z - Kc^2 + F(x, t)$$

was expressed as a difference equation and solved numerically for $c(x,t)$. The second term on the right describes the energy pooling reaction; the third term is an $O_2{}^1\Delta$ generation function. A simple Arrhenius form for $O_2{}^1\Delta$ release

$$F(x,t) = A\, e^{-E_a/RT}\, (EP(t))$$

from the endoperoxide film into the gas phase at $X = 0$ was used with the pre-exponential and activation energy parameters estimated from thermogravimetric data. $EP(t)$ is the density of endoperoxide (molecules/cm^2) in the thin film. $F(x,t)$ is a function of endoperoxide film temperature (which itself is a function of time). Finally, the numerical solution for $c(x,t)$ was squared and integrated over x to give a number proportional to the dimol emission signal. A comparison between calculated signal and experimental data is shown in Figure 6.

A final step was taken to determine the absolute magnitude of the calculated signal. The computer calculations were found to be a sensitive function of temperature, which is determined by the energy discharged through the circuit, the diffusion parameters, and the parameters chosen for the Arrhenius $O_2{}^1\Delta$ release rate. The latter quantities were obtained from thermogravimetric analysis and can not be said to be well determined. Therefore, the absolute scale for our calculated signal was chosen using the following procedure. An endoperoxide sample was deposited on the Nesatron substrate and pulse heated three times. The dimol emission signal was recorded for each release of $O_2{}^1\Delta$. The energy of discharge (the same for all three experiments) was considered an adjustable parameter in the modeling calculations and was chosen in such a manner that the calculated peak signal

decreased from one pulsed discharge to the next in the same proportions as the measured signal peak. This procedure is equivalent to compensating for poorly determined A and E_a in the Arrhenius expression by changing the temperature and allowing the discharge energy parameter to carry the experimentally determined information. Table 1 shows this comparison. The fitting criteria are satisfied with a discharge energy of 1.68 J/cm^2, a number which is less than 10% different from the value suggested by the apparent capacitor voltage and the measured effective area of the Nesatron plate. The fit is sensitive to 0.01 J/cm^2 change.

Along with the forced agreement of the proportionate fall off in peak dimol emission signal comes not only a remarkably good fit of the time profile of the emission signal (Figure 6) but good agreement with the absolute numerical values of the emission signal (Table 1). The latter implies that close to 100% of the released oxygen is in the singlet delta state.

The close agreement between the calculated signal time profile and the measured signal also implies that in fact $O_2{}^1\Delta$ is released into the gas phase (It would be difficult to model the signal decay curves if it is assumed that $O_2{}^1\Delta$ remains in and emits from the solid phase.) Separate experiments were performed in which a confining glass plate was introduced in front of the sample surface. If $O_2{}^1\Delta$ is emitted from the gas phase, we would expect to see a change in the signal once the gap between the sample and confining plate is reduced to values approximately equal to a diffusion distance (for times less than 10 ms). Indeed we see a large increase in signal for small gap distances (about 0.2 mm).

The excellent agreement between model and experiment, considering the simplicity of the model, leads to several conclusions: 1) the principle features of the experiment seem to be contained within the model, 2) there is no significant quenching other than energy pooling on the time scale of the experiment, and 3) virtually all of the oxygen being evolved is in the singlet delta state and is, in fact, released into the gas phase. Any alternative processes would be likely to lead to reduced signal levels and faster decays than those observed.

7

Table 1. Peak emission signals for a repetitively heated sample.

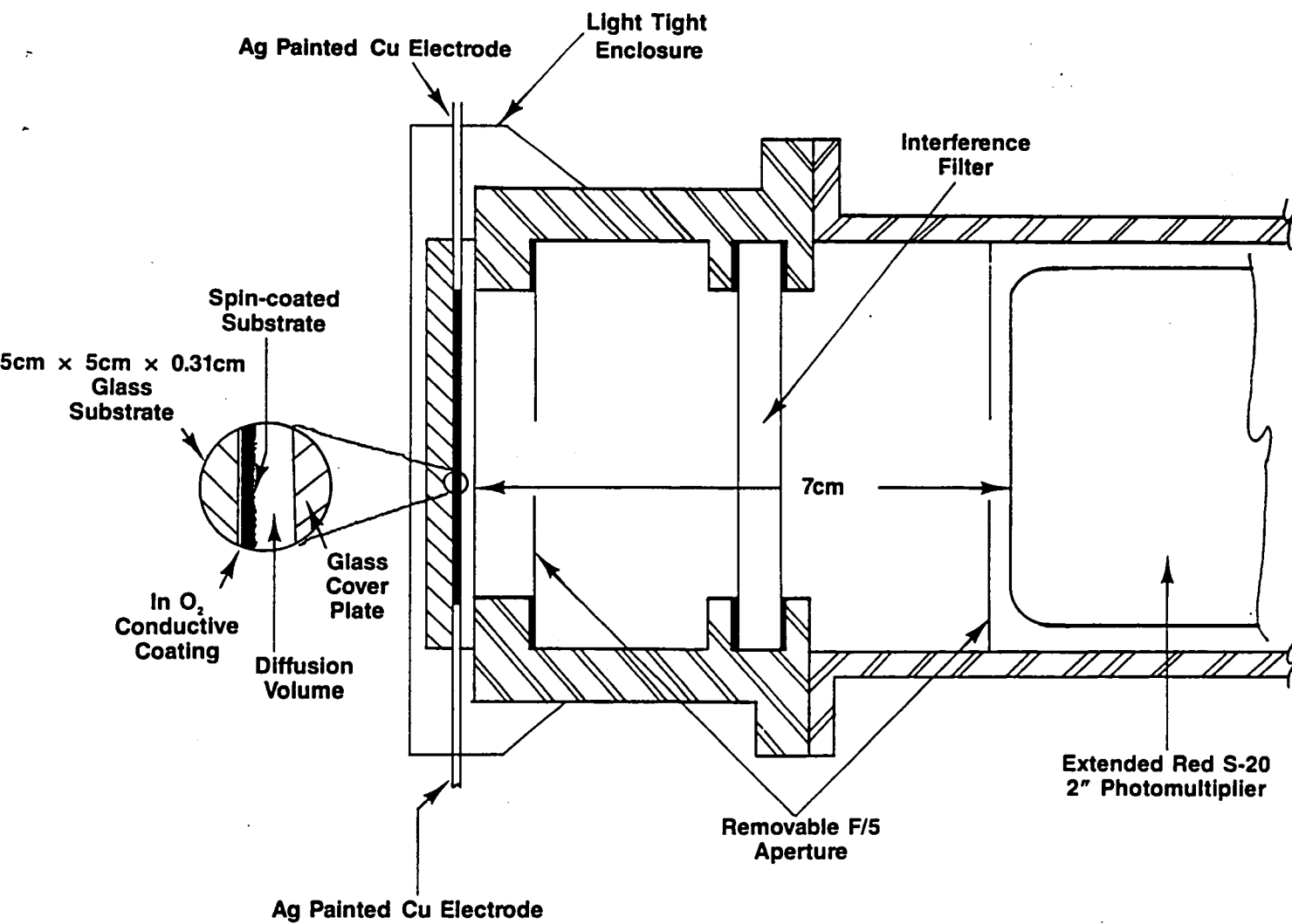|	Signal (volts)	
Expt. #	Model	Measured
1	.11	.11
2	.046	.046
3	.019	.028

Figure 1. Experimental Apparatus Used for Recent KMS Endoperoxide Studies.
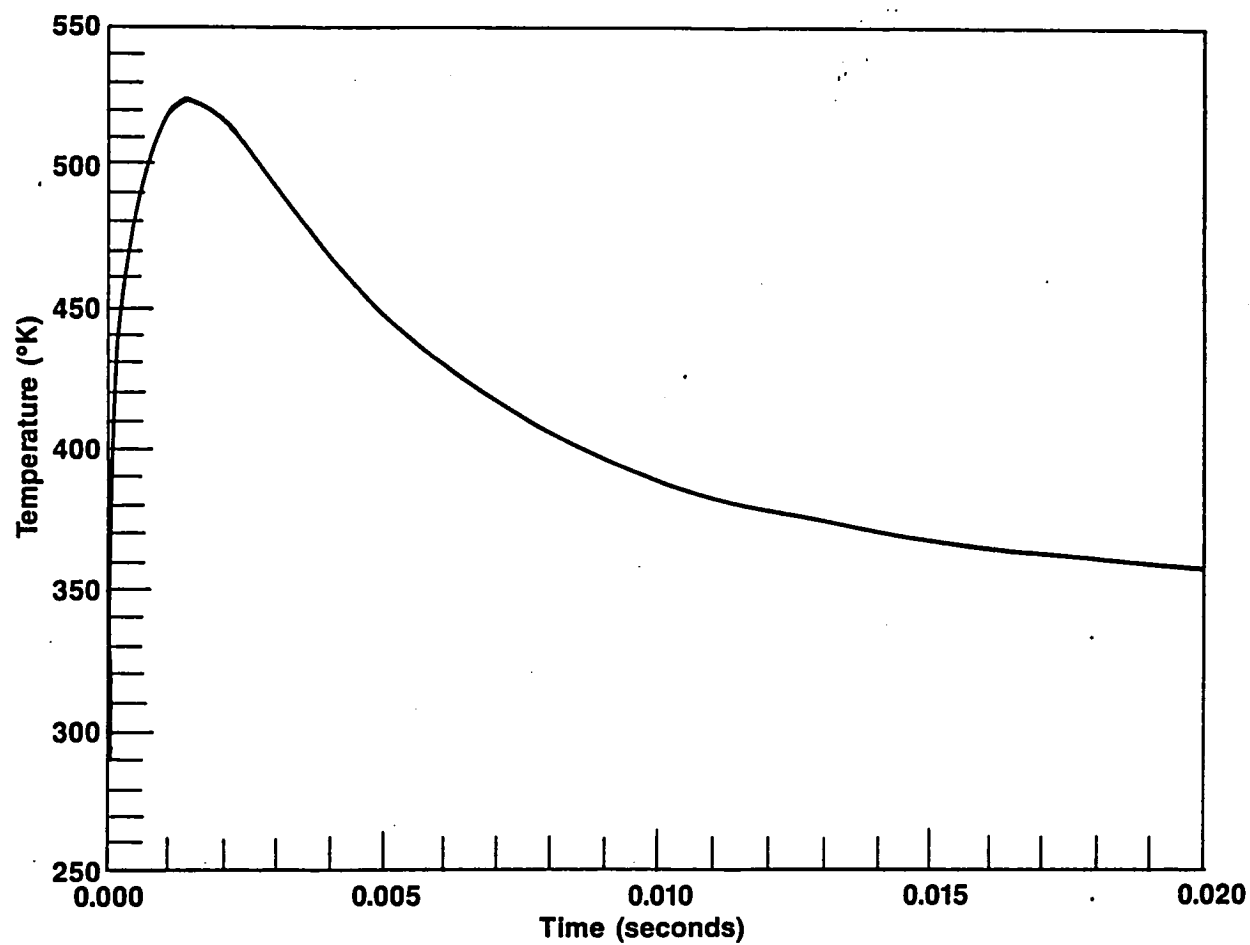
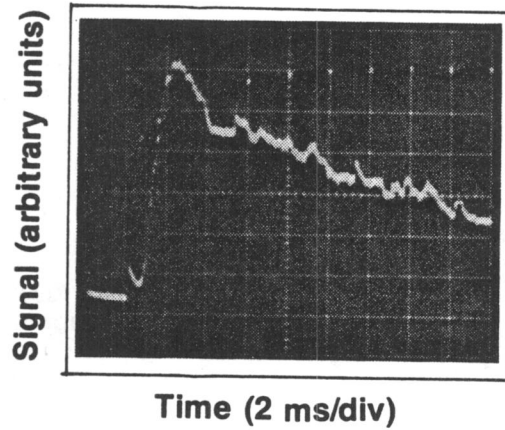Figure 2. Surface temperature of glass substrate.

Figure 3. Time-resolved Photomultiplier Signal. Interference Filter centered at 636.5 nm with Bandpass of 11 nm FWHM. Dimol Emission from spin-coated Endoperoxide film pulse-heated with 30J.
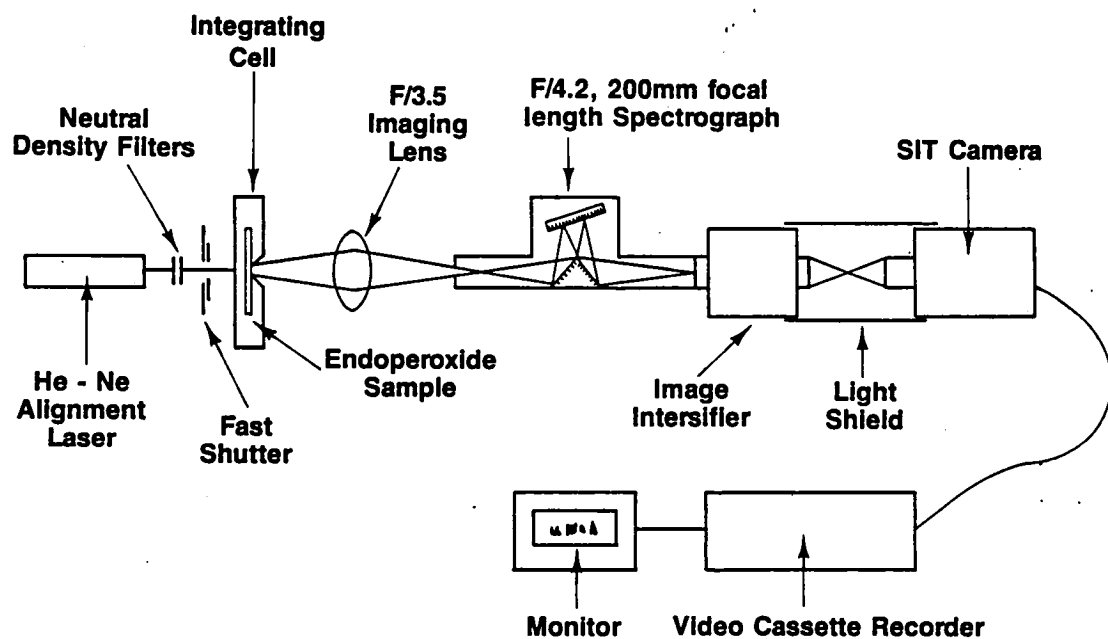
Figure 4. Experimental Apparatus for Spectrally Resolved Light Emission from Pulse-Heated Endoperoxide.
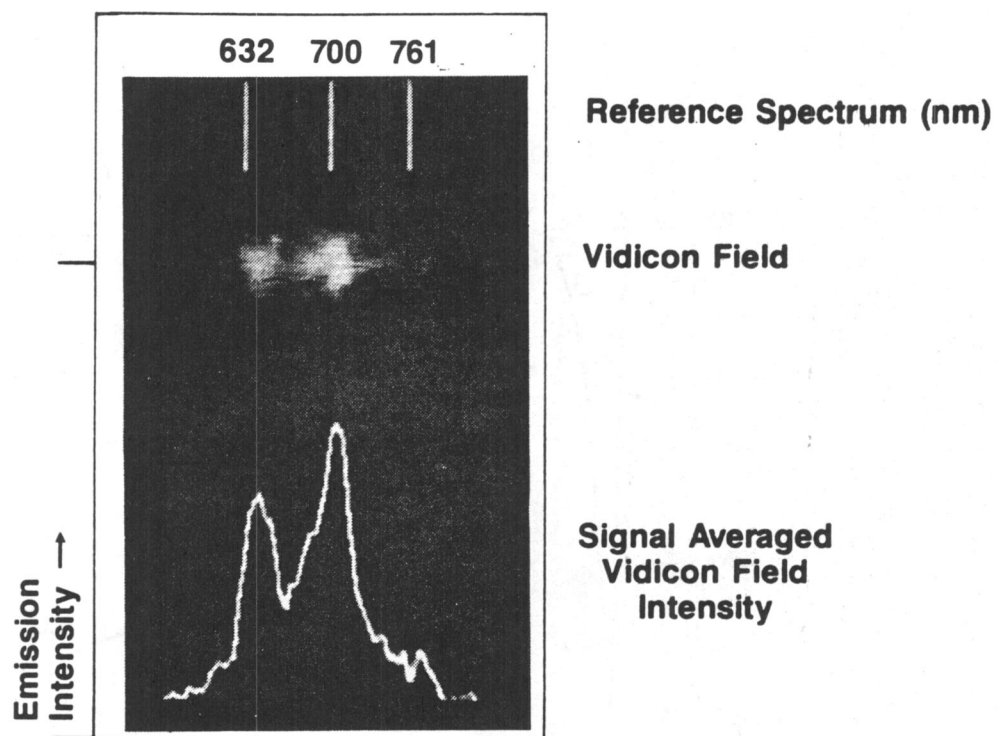
632   700   761   Reference Spectrum (nm)

Vidicon Field

Signal Averaged
Vidicon Field
Intensity

Emission Intensity →

Figure   5. Spectrally-resolved Emission from Spin-coated Endoperoxide film
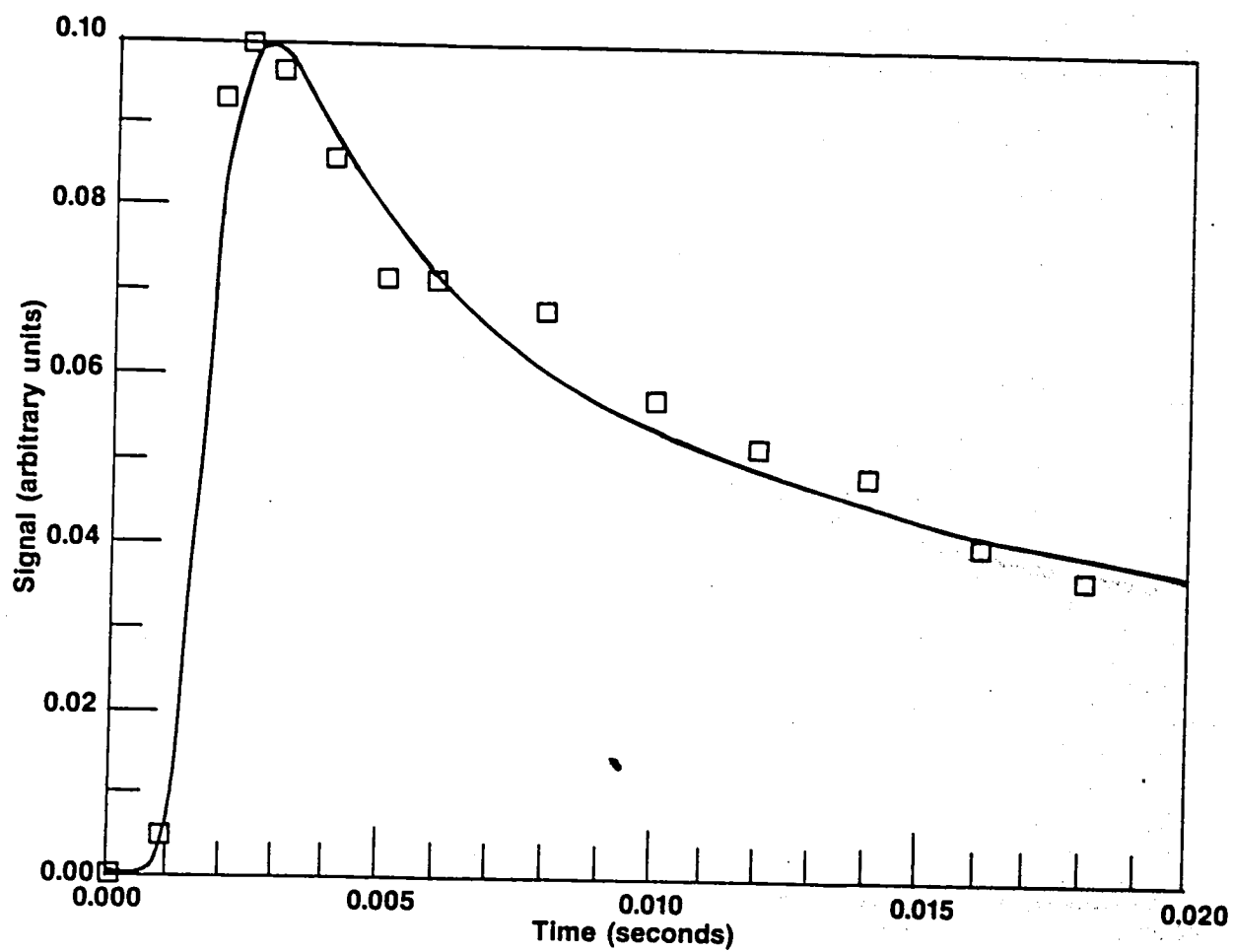pulse-heated with 44J.

Figure 6. dimol emission signal. □ - experimental data, solid curve-computer model.

TECHNICAL FEASIBILITY

The demonstration that $O_2{}^1\Delta$ can be efficiently released from thin films of solid endoperoxides is an important step in the development of a solar pumped iodine laser. A priori we were hopeful that $O_2{}^1\Delta$ would be able to diffuse through 100 Å films without significant quenching. The achievement of high yields from 1000 Å films is very encouraging, and the possibility now exists that even substantially thicker films could be used. This would ultimately translate into simpler system designs by relaxation of high surface area requirements.

A number of technical questions still need to be addressed before the feasibility of this approach to solar pumping of an iodine laser can be said to be demonstrated. Some questions still remain about $O_2{}^1\Delta$ release from endoperoxides; for example, can the high efficiencies and rapid release be maintained for materials with lower vapor pressures than those tested to date, so that no buffer gas would be required to prevent sublimation of endoperoxide upon heating. Of course, steps one and two of an integrated laser system remain to be investigated; namely, original $O_2{}^1\Delta$ generation by solid phase triplet sensitizers and transfer of $O_2{}^1\Delta$ to the acceptor material for formation of endoperoxide. The high degree of success in this Phase I feasibility study indicates that further research in these remaining areas is warranted.

1. Report No. NASA CR-172364	2. Government Accession No.	3. Recipient's Catalog No.
4. Title and Subtitle Singlet Oxygen Generator for a Solar Powered Chemically Pumped Iodine Laser		5. Report Date April 1984
		6. Performing Organization Code U-1462
7. Author(s) George E. Busch		8. Performing Organization Report No.
		10. Work Unit No.
9. Performing Organization Name and Address KMS Fusion, Inc. 3621 South State Road, P.O. Box 1567 Ann Arbor, Michigan 48106		11. Contract or Grant No. NAS1-17584
		13. Type of Report and Period Covered Contractor Report
12. Sponsoring Agency Name and Address National Aeronautics and Space Administration Washington, D. C. 20546		14. Sponsoring Agency Code

15. Supplementary Notes

Langley Technical Monitor: Dr. Edmund J. Conway
Final Report

16. Abstract

An experimental study was conducted to determine the potential of solid phase endoperoxides as a means to produce singlet-delta oxygen in the gas phase in concentrations useful to chemical oxygen-iodine lasers. The 1,4 - endoperoxide of ethyl 3- (4-methyl - 1-naphthyl) propanoate was deposited over an indium-oxide layer on a glass plate. Singlet-delta oxygen was released from the endoperoxide upon heating the organic film by means of an electrical discharge through the conductive indium oxide coating. The evolution of singlet-delta oxygen was determined by measuring the dimol emission signal at 634 nm.

Comparison of the measured signal with an analytic model leads to two main conclusions: 1) virtually all the oxygen being evolved is in the singlet-delta state and in the gas phase, and 2) there is no significant quenching other than energy pooling on the time scale of the experiment (~10 msec).

The use of solid-phase endoperoxide as a singlet-delta oxygen generator for an oxygen-iodine laser appears promising.

17. Key Words (Suggested by Author(s)) Singlet Oxygen Iodine Laser Endoperoxide	18. Distribution Statement Unclassified - unlimited Subject Category 20

19. Security Classif. (of this report) Unclassified	20. Security Classif. (of this page) Unclassified	21. No. of Pages 16	22. Price A02